ready apparent at 6 AU, this estimate must be considered as highly uncertain.

In many respects, Hale-Bopp resembles SW1. Both display activity when far from the sun (*23*), both show optical dust jets indicating anisotropic mass loss from the nucleus, and both are prodigious sources of CO [2000 kg s^{-1} for SW1 (*5*, *6*)]. However, whereas SW1 has a nearly circular trans-Jovian orbit that prevents a close approach to the sun, the orbit of Hale-Bopp is highly eccentric, and the solar insolation at the nucleus will increase by a factor of 50 between now and perihelion. Thus, Hale-Bopp provides an unprecedented opportunity to study the development of CO and H_2O outgassing in a comet that is still far from perihelion.

REFERENCES AND NOTES

1. F. Whipple, *Astrophys. J.* **111**, 375 (1950).
2. H. Matthews, D. Jewitt, M. Senay, *Int. Astron. Union Circ. 6234* (21 September 1995).
3. H. Rauer *et al.*, *Int. Astron. Union Circ. 6236* (25 September 1995).
4. D. C. Jewitt, in *Comets In The Post-Halley Era*, R. Newburn, M. Neugebauer, J. Rahe, Eds. (Kluwer, Dordrecht, 1991), pp. 19–65.
5. M. Senay and D. Jewitt, *Nature* **371**, 229 (1994).
6. J. Crovisier *et al.*, *Icarus* **115**, 213 (1995).
7. J. Luu and D. Jewitt, *Astron. J.* **100**, 913 (1990).
8. M. Womack, S. A. Stern, M. Festou, *Int. Astron. Union Circ. 6276* (21 December 1995).
9. W. F. Huebner, J. J. Keady, S. P. Lyon, *Solar Photo Rates for Planetary Atmospheres and Atmospheric Pollutants* (Kluwer, Dordrecht, 1992), p. 273.
10. J. Crovisier *et al.*, abstract at 27th Annual Meeting of the American Astronomical Society Division for Planetary Sciences, Kona, Hawaii, 9 to 13 October 1995.
11. J. Crovisier and J. Le Bourlot, *Astron. Astrophys.* **123**, 61 (1983).
12. F. P. Schloerb, M. J. Claussen, L. Tacconi-Garman, *ibid.* **187**, 469 (1987).
13. H. U. Keller *et al.*, *ibid.*, p. 807.
14. D. C. Boice, W. F. Huebner, S. A. Stern, in *Workshop on the Activity of Distant Comets*, W. Huebner *et al.*, Eds. (Southwest Research Institute Press, San Antonio, TX, 1993), pp. 134–139.
15. M. Bailey *et al.*, in preparation.
16. R. H. McNaught, *Int. Astron. Union Circ. 6198* (2 August 1995).
17. P. Eberhardt *et al.*, *Astron. Astrophys.* **187**, 481 (1987).
18. N. H. Samarasinha and M. Belton, *Icarus* **108**, 103 (1994).
19. J. Davies, T. Geballe, D. Cruikshank, T. Owen, C. de Bergh, *Int. Astron. Union Circ. 6225* (11 September 1995).
20. M. Hicks, *Int. Astron. Union Circ. 6200* (3 August 1995).
21. M. A'Hearn, D. G. Schleicher, P. D. Feldman , R. L. Millis, D. T. Thompson, *Astron. J.* **89**, 579 (1984).
22. D. Prialnik, *Adv. Space Res.* **9**, 25 (1989).
23. D. C. Jewitt, *Astrophys. J.* **351**, 277 (1990).
24. Thermodynamic parameters of the ices were taken from G. N. Brown and W. T. Ziegler, *Adv. Cryog. Eng.* **25**, 662 (1979). The Bond albedo and emissivity were taken to be 0.04 and 1.0, respectively. Thermal conduction was neglected: its effects would decrease the sublimation fluxes relative to the values plotted here. Neither the rotation state of the Hale-Bopp nucleus nor the conductivity of its surface materials are known.

25. We thank the JCMT operators for help observing, K. Chambers for the image in Fig. 1, and D. Tholen for providing perturbed ephemerides. D.J. appreciates support from the National Aeronautics and Space Administration's Origins of Solar Systems Program.

26 December 1995; accepted 1 February 1996

Imitation of *Escherichia coli* Aspartate Receptor Signaling in Engineered Dimers of the Cytoplasmic Domain

Andrea G. Cochran* and Peter S. Kim

Transmembrane signaling by bacterial chemotaxis receptors appears to require a conformational change within a receptor dimer. Dimers were engineered of the cytoplasmic domain of the *Escherichia coli* aspartate receptor that stimulated the kinase CheA in vitro. The folding free energy of the leucine-zipper dimerization domain was harnessed to twist the dimer interface of the receptor, which markedly affected the extent of CheA activation. Response to this twist was attenuated by modification of receptor regulatory sites, in the same manner as adaptation resets sensitivity to ligand in vivo. These results suggest that the normal allosteric activation of the chemotaxis receptor has been mimicked in a system that lacks both ligand-binding and transmembrane domains. The most stimulatory receptor dimer formed a species of tetrameric size.

Bacterial chemotaxis, the regulated swimming behavior of bacteria in an attractant or repellent gradient, is one of the most thoroughly studied and biochemically defined signaling processes (*1*, *2*). Determination of the structures of the dimeric ligand-binding domain of the *Salmonella typhimurium* aspartate receptor in apo and aspartate-bound forms was an important step toward understanding the transmembrane signaling mechanism (*3*). However, it is not obvious from these structures how periplasmic ligand binding triggers events in the cytoplasm. Aspartate binding induces only a small rotation of ~4° between monomers (about an axis parallel to the membrane and perpendicular to the twofold symmetry axis). Consistent with this structural view, disulfide cross-linking and nuclear magnetic resonance studies suggest that ligand binding results in small shifts in the relative positions of the transmembrane helices (*4*, *5*). Several types of interhelical motion have been suggested as possible signaling mechanisms: Examples include pistonlike movements, scissoring motions, and supercoiling of helices (*4*). Presumably, these adjustments in helix orientation reach the cytoplasmic portion of the receptor and are transmitted through the adapter protein CheW to the kinase CheA, thereby inhibiting phosphorylation of the diffusible messenger CheY (Fig. 1).

To extend structural and mechanistic studies to the cytoplasmic receptor-kinase complex, we engineered dimers of the *E. coli* aspartate receptor (Tar) cytoplasmic domain in which the monomers are held in parallel, as in the intact receptor (Fig. 1). The desired orientation was achieved by fusing the receptor domain to the short, parallel coiled-coil dimerization domain (leucine zipper) from the transcriptional activator GCN4 (*6*, *7*). In addition to providing a dimerization domain, the GCN4 peptide replaces the receptor sequence that presumably relays transmembrane conformational changes to the cytoplasm (*8*). Fusion to a stable, inflexible structural element fixes the structure of the receptor fragment in this critical region.

No detailed structural information is available to guide the design of a dimer of the Tar cytoplasmic domain. However, clues can be found in two cytoplasmic regions of the receptor that are associated with the process of adaptation (*1*, *2*).

Efficient gradient sensing requires continuous adjustment of receptor sensitivity. Attractant stimulation induces a net increase in methylation of four specific glutamic acid side chains (Fig. 2A), catalyzed by the methyl transferase CheR. Methylation of these glutamic acids, or mutation to glutamine, desensitizes the receptor to attractant ligands (*9*–*11*). Conversely, loss of attractant stimulation results in net demethylation by the methyl esterase CheB. The kinase activity of receptor-associated CheA, in the absence of ligand, increases in direct response to increases in receptor methylation or amidation (*11*–*13*), suggesting that structural changes related to receptor adaptation are intimately linked to the conformational changes that occur during receptor signaling.

The primary sequences of both methylation regions (K1 and R1; Fig. 2A) conform to seven-residue repeating patterns (4-3 hydrophobic repeats) typical of α-helical coiled coils (*2*, *14*). The seven-residue spacing of the three K1 methylation sites would align them on one face of a coiled-coil helix (*2*). Receptor point mutations that transform cells to an extreme smooth-swimming phe-

Howard Hughes Medical Institute, Whitehead Institute for Biomedical Research, Department of Biology, Massachusetts Institute of Technology, Nine Cambridge Center, Cambridge, MA 02142, USA.

*To whom correspondence should be addressed.

notype (*15*) also occur within the predicted K1 coiled-coil sequence and map to the face of the helix opposite the methylation sites. The segregation of these sites to discrete helical faces suggests that changes in kinase activity might result from modulating the exposure of the two faces, possibly by rotation of the K1 helices about each other in the receptor dimer. In contrast to typical dimeric coiled coils (*6, 16*), not two but four adjacent heptad positions of the Tar coiled coils would be largely uncharged, again suggesting that the relative orientation of the two monomers might not be fixed.

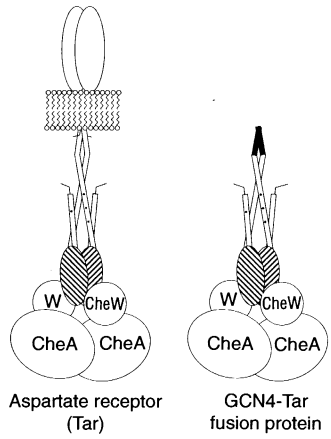

Fig. 1. Model for the chemotaxis signaling complex (left) and an analogous complex formed from a soluble dimer of the receptor cytoplasmic domain (right). The coiled-coil peptide dimerization domain of GCN4 is shown in black. Chemotactic signaling is thought to occur in a stable complex consisting of receptor dimer; two molecules of an essential adapter protein, CheW; and a dimeric histidine autokinase, CheA (*1, 12, 35, 36*). Phosphoryl transfer from CheA to CheY initiates a signal for clockwise flagellar rotation (tumbling) that is inactivated by hydrolysis of CheY phosphate. Binding of an attractant ligand by the receptor inhibits kinase activity (*20*), producing smooth-swimming behavior. The receptor subdomain shown as striped is the highly conserved "signaling" domain that is characteristic of the chemotaxis receptors (*32*). The white rods represent predicted α-helical coiled-coil domains (*2, 14*) in which receptor methylation sites (dots) are present.

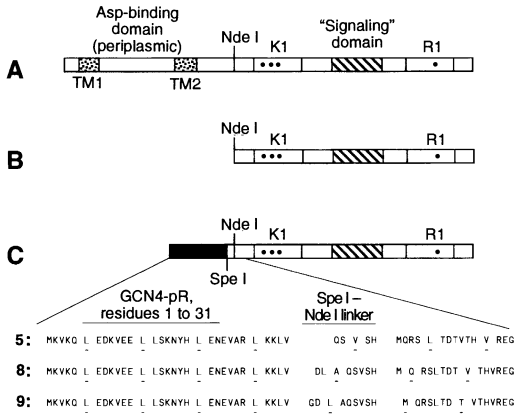

Fig. 2. Arrangement of domains in the *E. coli* aspartate receptor (Tar) and chimeras. (**A**) Full-length receptor. TM1 and TM2 indicate the first and second transmembrane segments, which flank the periplasmic ligand-binding domain. K1 and R1 indicate predicted α-helical coiled-coil domains (*2, 14*) that include four regulatory methylation sites (dots). The striped domain is the conserved signaling domain (Fig. 1). (**B**) Cytoplasmic domain of Tar, residues 257 to 553 (c-fragment) (*33, 34*). (**C**) Chimeras of Tar and the GCN4 dimerization domain (GCN4-pR) (*6, 17*). The amino acid sequences of the NH_2-terminal extensions of Tar are shown in an expanded view. Residues in the **d** position (leucines) of the GCN4 peptide, and Tar residues in heptad register, are underlined. The dimer designations **5**, **8**, and **9** indicate the number of amino acids from Tar encoded by the linker spanning the Spe I and Nde I restriction sites. Abbreviations for the amino acid residues are A, Ala; D, Asp; E, Glu; G, Gly; H, His; K, Lys; L, Leu; M, Met; N, Asn; Q, Gln; R, Arg; S, Ser; T, Thr; V, Val; and Y, Tyr.

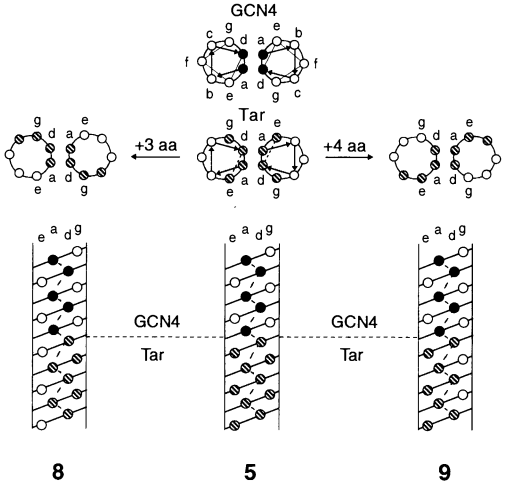

Fig. 3. Helical wheel (**top**) and helical net (**bottom**) representations of dimers **5**, **8**, and **9** in the region of the fusion junction. The helical wheel for the parallel, dimeric GCN4 coiled coil (*6, 16*) is shown at top center for comparison. The seven-residue (heptad) repeat is represented by the letters **a** through **g** on the wheel, where hydrophobic residues at positions **a** and **d** (black) constitute the dimer core. Four heptad positions of the predicted coiled coils of the receptor would be largely uncharged and are shown as striped. The helical net (positions **a**, **d**, **e**, and **g** only) is shown from the perspective of the supercoil axis of the GCN4 peptide. A continuous helix is assumed between domains [see also (*37*)]; aa, amino acid.

Fusion proteins designated **5**, **8**, and **9** were constructed (Fig. 2C) (*17*). The three fusion points were chosen in order to place the hydrophobic face of the GCN4 peptide in register with each of the three potential receptor dimer interfaces (Fig. 3). In dimer **5**, the four uncharged heptad positions of a Tar helix would be centered about the GCN4 dimer interface. In dimers **8** and **9**, these Tar residues would be shifted to either side of the peptide-defined dimer interface. It was expected that the large folding free energy (>10 kcal/mol) of the GCN4 peptide dimer (*18*) would be sufficient to distort the receptor dimer away from any intrinsic interface preferences in the region of the fusion junction. Because sensitivity to ligand is determined by the methylation state of the intact receptor, the three dimers, as well as the monomer that lacks the leucine zipper (c-fragment) (Fig. 2B), were each prepared with the wild-type methylation site sequence of QEQE and as the two extreme adapted forms EEEE and QQQQ (*19*).

To determine whether dimerization of the Tar cytoplasmic domain yields a functional substitute for the receptor dimer, we assayed in vitro phosphorylation as described for full-length, vesicle-bound Tar (*11, 20–22*). At receptor concentrations used here (20 μM), dimer **5** stimulated phosphorylation of CheY, whereas the c-fragment did not (Fig. 4A) (*23*). The extent of kinase activation by the dimer depended on the methylation site sequence, in the manner reported for full-length Tar in membrane vesicles (*11*). These results suggest that the structure of the GCN4-linked dimer approximates that of the native receptor.

The receptor dimer was sensitive to distortion of the dimer interface, as demonstrated by differences in CheA activation by the QEQE forms of dimers **5**, **8**, and **9** (Fig. 4B). QEQE-**8** did not stimulate phosphorylation, whereas QEQE-**9** had a marked stimulatory effect. QEQE-**5** was intermediate in its activity (*24*). The activity differences (**9** > **5** > **8**) are not correlated with the length of the interdomain linker, but instead appear to correlate with rotation of the dimer interface (Fig. 3). Mutation of the methylation site residues to either EEEE or QQQQ attenuated the effect of the linkage variation. All three EEEE dimers were inactive, whereas the QQQQ dimers activated CheA. Therefore, although kinase activation by the QEQE dimers is sensitive to linkage point, none of the linkages was incompatible with the formation of an active kinase complex. The lack of sensitivity to the interface perturbation at the two extreme methylation states resembles the adaptation to signal that occurs in full-length Tar.

The molecular masses of the nine Tar

dimers were determined by analytical ultracentrifugation (Fig. 5) (*25*). The observed apparent molecular masses suggest that the dimer **9** variants formed tetramers at the sample concentration of 5 μM. This effect was independent of the glycerol present in kinase assay buffers. Dimer **8** aggregated to a lesser extent, and, in this instance, the effect was enhanced by glycerol. However, the rank order of aggregation tendency for the isolated receptor variants (**9** > **8** > **5**) does not correlate with the extent of CheA activation induced by the QEQE dimers.

Regulation of CheA activity is the immediate consequence of attractant binding to the chemotaxis receptors. Accordingly, any model for conformational changes in the receptor periplasmic and transmembrane domains must be compatible with the properties of the cytoplasmic signaling complex. Soluble dimers of the Tar cytoplasmic domain are kinase activators in vitro (Fig. 4A); membrane is not essential. Furthermore, dimerization of the receptor cytoplasmic domain is necessary but insufficient for kinase activation (Fig. 4B); correct orientation of the monomers is important. Desensitization to ligand-induced conformational change by alteration of receptor methylation (or amidation) is critical for bacteria to adapt to a constant stimulus. The linkage-induced distortions in dimers **5**, **8**, and **9** are subject to a similar process, indicating that the conformational differences among these dimers resemble those that occur naturally in the intact Tar dimer. Although we do not yet know the high-resolution structural effects of varying the interdomain linkage, the observed pattern is consistent with activation either by rotation (or supercoiling) of roughly parallel helices about a twofold axis or by a small pivot between monomer subunits. Signaling models that require an asymmetric translation of monomers normal to the membrane (piston model), or a conformational change solely within a monomer subunit (*26*), appear less likely.

Ligand-induced oligomerization of receptors has emerged as a general mechanism of intracellular kinase activation (*27*). This mechanism is demonstrated in the crystal structures of human growth hormone (*28*) and tumor necrosis factor (*29*) bound to the extracellular domains of their receptors. Other receptors, such as Tar and the insulin receptor (*30*), are dimeric even in the absence of ligand; these receptors are thought to signal by transmitting specific conformational changes across the membrane to the interior of the cell. The responsiveness of the dimerized Tar cytoplasmic domain to the applied strain at its NH_2-terminus demonstrates that productive conformational change could indeed be propagated through a small number of transmembrane helices. However, the observation that chemotaxis receptors form clusters at the poles of *E. coli* (*31*) suggests that aggregation may also play a role in signaling by these dimeric receptors. Although prokaryotic and eukaryotic signaling mechanisms are typically described as one of the two extremes of transmembrane conformational change or receptor oligomerization, the two mechanisms may be coupled to amplify extracellular signals.

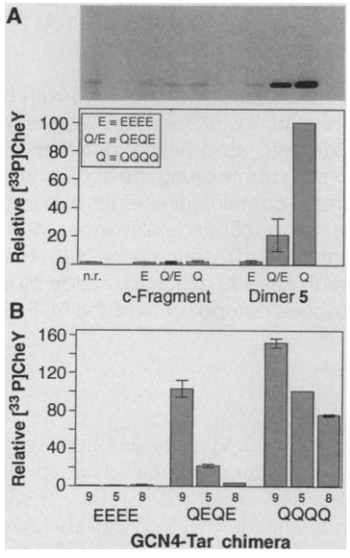

Fig. 4. Kinase activation in the presence of the Tar c-fragment or GCN4 chimeras. (**A**) Comparison of the activities of the Tar c-fragment and dimer **5** as a function of methylation site sequence. Lane 1, no added receptor (n.r.); lanes 2 to 4, c-fragment (20 μM) in the EEEE, QEQE, and QQQQ configurations, respectively; and lanes 5 to 7, dimer **5** (20 μM) in the EEEE, QEQE, and QQQQ configurations, respectively. The radioactive band is CheY phosphate produced in the reaction (*22*). The intensity of the bands, as a percentage of the intensity observed for QQQQ-**5** (lane 7), is shown below; data are means ± SD of duplicate experiments. (**B**) Comparison of the activities of the methylation site variants of dimers **5**, **8**, and **9** (20 μM, as indicated). Data represent the relative intensities of the CheY phosphate bands (QQQQ-**5** = 100%) and are expressed as means ± SD of duplicate experiments.

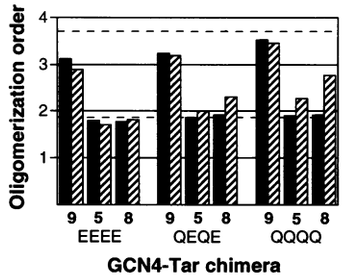

Fig. 5. Analytical ultracentrifugation of the nine Tar dimers at pH 7.5 in the presence (striped bars) or absence (black bars) of 10% (w/v) glycerol (*25*). The lane order is the same as that of Fig. 4B. Data are expressed as the ratio of reduced apparent molecular weight (σ) to that calculated for the monomer. The dotted lines indicate σ values that appear to correspond to dimers and tetramers at 1.85 and 3.7 times the calculated monomer value, respectively.

REFERENCES AND NOTES

1. R. C. Stewart and F. W. Dahlquist, *Chem. Rev.* **87**, 997 (1987); R. B. Bourret, K. A. Borkovich, M. I. Simon, *Annu. Rev. Biochem.* **60**, 401 (1991); J. B. Stock, M. G. Surette, W. R. McCleary, A. M. Stock, *J. Biol. Chem.* **267**, 19753 (1992); J. S. Parkinson, *Cell* **73**, 857 (1993).
2. J. B. Stock, G. S. Lukat, A. M. Stock, *Annu. Rev. Biophys. Biophys. Chem.* **20**, 109 (1991).
3. M. V. Milburn *et al.*, *Science* **254**, 1342 (1991); J. I. Yeh, H.-P. Biemann, J. Pandit, D. E. Koshland Jr., S.-H. Kim, *J. Biol. Chem.* **268**, 8789 (1993); W. G. Scott *et al.*, *J. Mol. Biol.* **232**, 555 (1993); J. U. Bowie, A. A. Pakula, M. I. Simon, *Acta Crystallogr.* **D51**, 145 (1995).
4. Reviewed in B. L. Stoddard and W. G. Scott, *Structure* **2**, 877 (1994).
5. M. A. Danielson, H.-P. Biemann, D. E. Koshland Jr., J. J. Falke, *Biochemistry* **33**, 6100 (1994); G. L. Lee, M. R. Lebert, A. A. Lilly, G. L. Hazelbauer, *Proc. Natl. Acad. Sci. U.S.A.* **92**, 3391 (1995); S. A. Chervitz and J. J. Falke, *J. Biol. Chem.* **270**, 24043 (1995); S. A. Chervitz, C. M. Lin, J. J. Falke, *Biochemistry* **34**, 9722 (1995); I. N. Maruyama, Y. G. Mikawa, H. I. Maruyama, *J. Mol. Biol.* **253**, 530 (1995).
6. E. K. O'Shea, R. Rutkowski, P. S. Kim, *Science* **243**, 538 (1989); J. C. Hu, E. K. O'Shea, P. S. Kim, R. T. Sauer, *ibid.* **250**, 1400 (1990).
7. Recent studies have described the use of coiled coils to assemble domains of three transmembrane receptors: the heterodimeric extracellular domain of the T cell receptor [H.-C. Chang *et al.*, *Proc. Natl. Acad. Sci. U.S.A.* **91**, 11408 (1994)], a trimer of the ligand-binding portion of the interleukin-2 receptor β chain [Z. Wu *et al.*, *Protein Eng.* **7**, 1137 (1994)], and a semisynthetic heterodimer of the cytoplasmic tails of the integrin $\alpha_{IIb}\beta_3$ receptor [T. W. Muir, M. J. Williams, M. H. Ginsburg, S. B. H. Kent, *Biochemistry* **33**, 7701 (1995)].
8. L. A. Collins, S. M. Egan, V. Stewart, *J. Bacteriol.* **174**, 3667 (1992); J. W. Baumgartner *et al.*, *ibid.* **176**, 1157 (1994); T. Jin and M. Inouye, *J. Mol. Biol.* **244**, 477 (1994).
9. P. Dunten and D. E. Koshland Jr., *J. Biol. Chem.* **266**, 1491 (1991).
10. C. Park, D. P. Dutton, G. L. Hazelbauer, *J. Bacteriol.* **172**, 7179 (1990).
11. K. A. Borkovich, L. A. Alex, M. I. Simon, *Proc. Natl. Acad. Sci. U.S.A.* **89**, 6756 (1992).
12. S. C. Schuster, R. V. Swanson, L. A. Alex, R. B. Bourret, M. I. Simon, *Nature* **365**, 343 (1993).
13. E. G. Ninfa, A. Stock, S. Mowbray, J. Stock, *J. Biol. Chem.* **266**, 9764 (1991).
14. A. Lupas, M. Van Dyke, J. Stock, *Science* **252**, 1162 (1991). An improved coiled-coil prediction algorithm based on pairwise residue correlations [B. Berger *et al.*, *Proc. Natl. Acad. Sci. U.S.A.* **92**, 8259 (1995)] scores both K1 (56% likelihood, residues 294 to 323) and R1 (59% likelihood, residues 487 to 516) regions as probable coiled coils.
15. Tar point mutations that result in extreme signaling phenotypes [N. Mutoh, K. Oosawa, M. I. Simon, *J. Bacteriol.* **167**, 992 (1986)] generally occur on one face of a putative K1 helix that extends toward the conserved signaling domain (Fig. 2A), or in a reciprocal pattern extending from the R1 methylation domain back to the signaling domain. An analogous class of serine receptor (Tsr) mutations [P. Ames and J. S. Parkinson, *Cell* **55**, 817 (1988)] exhibits the same pattern.
16. E. K. O'Shea, J. D. Klemm, P. S. Kim, T. Alber, *Science* **254**, 539 (1991); E. K. O'Shea, R. Rutkowski, P. S. Kim, *Cell* **68**, 699 (1992); E. K. O'Shea, K. J. Lumb, P. S. Kim, *Curr. Biol.* **3**, 658 (1993); C.

Cohen and D. A. D. Parry, *Proteins* **7**, 1 (1990).
17. DNA encoding the Tar c-fragment (residues 257 to 553) (Fig. 2B) (*32, 33*) was ligated into the T7 expression vector pAED4 [D. S. Doering, thesis, Massachusetts Institute of Technology (1992)] according to standard molecular cloning protocols [J. Sambrook, E. F. Fritsch, T. Maniatis, *Molecular Cloning: A Laboratory Manual* (Cold Spring Harbor Laboratory, Cold Spring Harbor, NY, ed. 2, 1989)]. The EEEE and QQQQ variants were obtained by in vitro mutagenesis (Amersham kit RPN 1523) of the c-fragment construct. An expression vector (p4LZ) encoding residues 2 to 33 of the GCN4 dimerization domain has been described [K. J. Lumb, C. M. Carr, P. S. Kim, *Biochemistry* **33**, 7361 (1994)]; the coding sequence was modified here to include two additional amino acids (Lys-Val) after the initiating methionine to yield plasmid pGCN4-pR (Fig. 2C). The encoded GCN4-pR peptide is fully folded as judged by its circular dichroism spectrum. The GCN4-Tar chimeras were obtained by joining the two constructs with short synthetic linkers encoding the sequences shown in Fig. 2C. Proteins were expressed in *E. coli* strain RP3098, from which the *che* genes have been deleted [R. S. Smith and J. S. Parkinson, *Proc. Natl. Acad. Sci. U.S.A.* **77**, 5370 (1980)]. The GCN4 fusion proteins were purified essentially as described for the c-fragment (*34*). Concentrations of dialyzed proteins were determined from their absorbance spectra in 6 M guanidine hydrochloride [H. Edelhoch, *Biochemistry* **6**, 1948 (1967)].
18. C. M. Carr, thesis, Massachusetts Institute of Technology (1995); J. A. Zitzewitz, O. Bilsel, J. Luo, B. E. Jones, C. R. Matthews, *Biochemistry* **34**, 12812 (1995).
19. The genes of the bacterial chemotaxis receptors encode a mixture of glutamic acid (E) and glutamine (Q) at the major cytoplasmic methylation sites. For Tar, the residues are Q295, E302, Q309, and E491, or QEQE, in the newly synthesized receptors (*32*).
20. K. A. Borkovich, N. Kaplan, J. F. Hess, M. I. Simon, *Proc. Natl. Acad. Sci. U.S.A.* **86**, 1208 (1989).
21. K. A. Borkovich and M. I. Simon, *Methods Enzymol.* **200**, 205 (1991); J. F. Hess, R. B. Bourret, M. I. Simon, *ibid.*, p. 188.
22. Chemotaxis proteins CheW, CheA, and CheY were produced from overexpression plasmids (*35*) and purified according to standard protocols (*21, 36*). Concentrations of purified proteins were determined as described (*17*). Each reaction mixture (10 μl final volume) contained the appropriate purified receptor fragment (20 μM), 2 μM CheW, 0.1 μM CheA, and 15 μM CheY in 50 mM tris-HCl (pH 7.5), 50 mM KCl, 5 mM $MgCl_2$, and 10% (w/v) glycerol. Protein mixtures were incubated for 6 hours at room temperature before initiation of the reaction by addition of 1 μl of 1 mM [γ-^{33}P]adenosine triphosphate (~10^4 cpm/pmol) (DuPont Biotechnology Systems). Reactions were quenched after 10 s by addition of 5 μl of 2× SDS loading buffer containing 25 mM EDTA (*21*), and the entire volume was applied (without heating) to denaturing 10% polyacrylamide–tricine gels (0.075 by 7 by 10 cm) [H. Schagger and G. von Jagow, *Anal. Biochem.* **166**, 368 (1987)]. After electrophoresis at 85 V, gels were stained with Coomassie blue, dried, and subjected to quantitative autoradiography (*21*) (FUJIX BAS 2000).
23. Kinase stimulation by tumble-mutant fragments of the *E. coli* serine receptor (Tsr) [P. Ames and J. S. Parkinson, *J. Bacteriol.* **176**, 6340 (1994)] requires a much higher fragment concentration than did kinase stimulation by soluble GCN4-Tar dimers. The protein concentrations used here (*22*) were identical to those used in assays of intact Tar in membrane vesicles (*11*) but included an approximately fivefold higher concentration of receptor; the extents of CheA stimulation were comparable.
24. Circular dichroism studies confirmed that all fusion proteins were folded and differed only slightly in secondary structure content at low temperatures. {The QQQQ variants [θ_{222} (mean residue ellipticity) = −23,000 degree cm^2 dmol^{-1} at 0°C] were somewhat more helical than the QEQE or EEEE variants (θ_{222} = −18,000 degree cm^2 dmol^{-1} at 0°C).} Thermal denaturation studies revealed a distinct transition midpoint for each interdomain linkage (with apparent midpoints of 52°, 57°, and 64°C, for the QEQE variants of **8**, **5**, and **9**, respectively, at 1.3 μM receptor), consistent with the idea that the receptor conformation has been strained by shifting the dimer interface. These midpoints were unaffected by methylation site mutations.
25. Samples (5 μM) were analyzed at 9000, 11,000, and 14,000 rpm in a Beckman XL-A centrifuge. Centrifuge temperature was 10°C for samples lacking glycerol and 20°C for those containing glycerol; sample buffer was 5 mM tris-HCl (pH 7.5), 50 mM KCl, and 5 mM $MgCl_2$. Data sets (six to eight per protein) were fitted simultaneously to a single-species model with the program NONLIN [M. L. Johnson, J. J. Correia, D. A. Yphantis, H. R. Halvorson, *Biophys. J.* **36**, 575 (1981)] to yield an apparent σ value. Expected monomer σ values were calculated with partial specific volumes based on amino acid composition as described [T. M. Laue, B. D. Shah, T. M. Ridgeway, S. L. Pelletier, in *Analytical Ultracentrifugation in Biochemistry and Polymer Science*, S. E. Harding, A. J. Rowe, J. C. Horton, Eds. (Royal Society of Chemistry, Cambridge, 1992), pp. 90–125].
26. D. L. Milligan and D. E. Koshland Jr., *Science* **254**, 1651 (1991).
27. Reviewed in C.-H. Heldin, *Cell* **80**, 213 (1995).
28. A. M. de Vos, M. Ultsch, A. A. Kossiakoff, *Science* **255**, 306 (1992); W. Somers, M. Ultsch, A. M. de Vos, A. A. Kossiakoff, *Nature* **372**, 478 (1994).
29. D. W. Banner *et al.*, *Cell* **73**, 431 (1993).
30. S. R. Hubbard, L. Wei, L. Ellis W. A. Hendrickson, *Nature* **372**, 746 (1994).
31. J. R. Maddock and L. Shapiro, *Science* **259**, 1717 (1993).
32. A. Krikos, N. Mutoh, A. Boyd, M. I. Simon, *Cell* **33**, 615 (1983).
33. K. Oosawa, N. Mutoh, M. I. Simon, *J. Bacteriol.* **170**, 2521 (1988).
34. N. Kaplan and M. I. Simon, *ibid.*, p. 5134; D. G. Long and R. M. Weis, *Biochemistry* **31**, 9904 (1992).
35. J. A. Gegner, D. R. Graham, A. F. Roth, F. W. Dahlquist, *Cell* **70**, 975 (1992).
36. J. A. Gegner and F. W. Dahlquist, *Proc. Natl. Acad. Sci. U.S.A.* **88**, 750 (1991).
37. W. T. Pu and K. Struhl, *ibid.*, p. 6901.
38. We thank F. W. Dahlquist for providing expression plasmids for CheA, CheW, and CheY; J. S. Parkinson for providing *E. coli* chemotaxis deletion strains; and K. M. Shokat and J. K. Judice for helpful comments on the manuscript. A.G.C. was supported by a National Science Foundation postdoctoral fellowship (CHE-9102242) and a Public Health Service training grant (T32 AI07348-07). This research was supported by the Howard Hughes Medical Institute.

2 August 1995; accepted 17 November 1995

Heparin Structure and Interactions with Basic Fibroblast Growth Factor

S. Faham, R. E. Hileman, J. R. Fromm, R. J. Linhardt,* D. C. Rees*

Crystal structures of heparin-derived tetra- and hexasaccharides complexed with basic fibroblast growth factor (bFGF) were determined at resolutions of 1.9 and 2.2 angstroms, respectively. The heparin structure may be approximated as a helical polymer with a disaccharide rotation of 174° and a translation of 8.6 angstroms along the helix axis. Both molecules bound similarly to a region of the bFGF surface containing residues asparagine-28, arginine-121, lysine-126, and glutamine-135; the hexasaccharide also interacted with an additional binding site formed by lysine-27, asparagine-102, and lysine-136. No significant conformational change in bFGF occurred upon heparin oligosaccharide binding, which suggests that heparin primarily serves to juxtapose components of the FGF signal transduction pathway.

Despite the importance of heparin and related glycosaminoglycans as components of the extracellular matrix, as participants in signal transduction pathways, and as therapeutic agents, atomic resolution structures are not available for heparin-based species larger than monosaccharides [reviewed in (*1*)]. This absence of precise structural information reflects difficulties in obtaining homogenous samples of heparin-derived molecules. The heparin polymer consists of a basic disaccharide repeat unit comprised of L-iduronic acid (Idu) and D-glucosamine (GlcN) joined by α(1→4) linkages (Fig. 1A). A typical heparin disaccharide contains a total of three sulfate groups: one attached to the 2-hydroxyl group of Idu and two linked to the 2-amino and 6-hydroxyl groups of GlcN. The related glycosaminoglycan heparan sulfate has a similar structure containing D-glucuronic acid, L-Idu, and D-GlcN but is less extensively sulfated. Successive disaccharides within heparin are related by a twofold screw operation, generated by a rotation angle of ~180° coupled to a translation of ~8.0 to 8.7 Å along the helix axis (*2*). The structure of heparin may be approximated by a ribbon with sulfate and carboxyl groups on the edges and hydroxyl and sugar ring oxygen atoms positioned on the surfaces between these negatively charged groups. Although the average structure of heparin is defined, local structural alterations exist within the heparin polymer that are a result of heterogeneity in the sequence, conforma-

S. Faham and D. C. Rees, Division of Chemistry and Chemical Engineering 147-75CH, California Institute of Technology, Pasadena, CA 91125, USA.
R. E. Hileman, J. R. Fromm, R. J. Linhardt, Division of Medicinal and Natural Products Chemistry, College of Pharmacy, University of Iowa, Iowa City, IA 52242, USA.

*To whom correspondence should be addressed. E-mail: rees@citray.caltech.edu and linhardt@blue.weeg.uiowa.edu